

Flexible Distributed Bragg Reflectors from Nanocolumnar Templates

Mauricio E. Calvo, Lola González-García, Julián Parra-Barranco, Angel Barranco, Alberto Jiménez-Solano, Agustín R. González-Elipe,* and Hernán Míguez*

Technological evolution of flexible optoelectronic devices, such as solar cells or light emitting diodes,^[1–6] must be accompanied by that of flexible optical and electronic materials in order to fulfill the increasing requirements of higher performance and functionality. In that regard, last years have seen a boost of the research in this field, a wide variety of approaches having been taken to prepare flexible components.^[7–11] Integration into devices will require stability of their properties upon bending and stretching, adaptability to different types of substrates, durability, etc.^[12] Among optical materials employed in optoelectronics, distributed Bragg reflectors (DBRs) play a central role as either photon frequency filters, optical cavities to enhance spontaneous or stimulated emission^[13] or simply as mirrors to increase the time of residence of photons in absorbing electrodes and thus improve their photovoltaic performance.^[14–16] In order to attain the flexible version of the classical stratified multilayer structure characteristic of DBRs, a common strategy is to stack thin polymer layers of alternate refractive index.^[17] Enhanced spontaneous emission has been observed from flexible optical cavities prepared based on this approach.^[18] Also, by rolling two polymers around a cylindrical core, tunable elastic optical multilayered fibers have been attained.^[19] However, elastomers usually possess low refractive indexes, typically comprised in a narrow range, so a small dielectric contrast is typically achieved. This means that a large number of layers must be stuck in order to reach intense reflections and only in narrow spectral ranges. One way to increase the refractive index contrast between layers relies on the deposition of hybrid precursors made of a mixture of polymers and higher refractive index inorganic particles.^[20] In this way, the refractive index contrast is increased, although its value is limited by the amount of particles that can be dispersed in the polymers. In addition, this approach requires a high degree of physicochemical compatibility of the particle surface with the polymer, or the strict control of the particle formation in a polymeric medium.^[21]

Recently, another alternative route to the use of purely polymeric structures to attain flexible Bragg mirrors, and in which enhanced dielectric contrast is achieved, has been successfully demonstrated.^[22,23] Such method takes advantage of multilayers possessing an open porous and interconnected network, which arises as a result of piling up layers of nanoparticles, to infiltrate a polymer that penetrates the multilayer structure. The polymer holds it together and, after the adequate treatment, permits the hybrid structure to be lifted off from the substrate. In this process, the optical quality of the originally deposited Bragg reflector is preserved. Just by controlling the thickness and the composition of the layers, this approach has been proven suitable to attain flexible DBRs of high reflectance intensity ($80\% < R < 100\%$) and spectral width ($\Delta\lambda/\lambda_{\text{MAX}} = 40\%$) in an ample range of optical wavelengths ($200 \text{ nm} < \lambda < 1500 \text{ nm}$). In principle, this method is applicable to any porous optical material not as rigid as to prevent the final hybrid structure to inherit the mechanical properties of the infiltrated polymer.

In this communication, we describe the preparation method and properties of a novel highly reflecting and flexible DBR. A porous nanocolumnar structure with photonic crystal properties, attained by oblique angle physical vapor deposition, is infiltrated by a polymer to achieve a new hybrid nanostructure that preserves a high dielectric constant contrast with improved mechanical properties. This type of multilayer structures has been previously used as optofluidic sensors to determine the concentration of liquid solutions or the proportion of two components in mixtures of liquids.^[24,25] Structural and optical characterization demonstrates the uniform infiltration of the polymer throughout the whole interstitial network of these porous multilayers, which is crucial to the realization of a robust self-standing structure. Such self-standing film could only be lifted off by depositing an intermediate layer of nanoparticles between the substrate and the porous photonic array, which both allows the growth of nanocolumns onto it and favors the detachment of the whole multilayer from the substrate after polymer infiltration.

Periodically alternated nanocolumnar arrays are typically grown on a variety of substrates by using physical vapor oblique angle deposition (PV OAD), in which the substrate is tilted with respect to the source of precursor species (known as *target*) in the chamber. A columnar nanostructure with open porosity results from the shadowing imposed by regions of faster growth over others.^[24,26,27] Porosities as high as 60%–70% of the total thin-film volume can be achieved by this procedure.^[28] This method has been employed in several occasions before to build porous DBRs.^[29,30] In our case, we use specifically the methods and experimental conditions reported

Dr. M. E. Calvo, Dr. L. González-García,^[†]
J. Parra-Barranco, Dr. A. Barranco, A. Jiménez-Solano,
Dr. Prof. A. R. González-Elipe, Prof. H. Míguez
Instituto de Ciencia de Materiales de Sevilla
Consejo Superior de Investigaciones
Científicas-Universidad de Sevilla
C/ Américo Vespucio 49, Sevilla 41092, Spain
E-mail: arge@icmse.csic.es; h.miguez@csic.es



^[†]Present Address: Leibniz-Institut für Neue Materialien GmbH Campus
D2 2, 66123 Saarbrücken, Germany

DOI: 10.1002/adom.201400338

in references.^[24,25] Full details can be found in the Experimental Section. In brief, porous silicon oxide and titanium oxide layers are deposited by PV OAD, control over the thickness and refractive index of the layers being achieved by varying the deposition time and the tilt angle, the latter affecting strongly the porosity of the final layer. The porous mirror is then embedded with polydimethyl siloxane oligomers (PDMS), which are polymerized in situ. This type of compound has been proven useful to infiltrate voids of nanometric size,^[22] and in particular the void network of nanocolumnar arrays,^[31] although no flexible structures were attained in that precedent.

Once ready, the hybrid structure must be lifted from the substrate to attain a self-standing mirror. Preserving the structural quality of a film that is mechanically detached from a surface depends on the surface tension at the interface between them. If it is too low, i.e., contact between film and substrate is favoured, the energy required to separate them may be too high and the coating might be harmed during extraction.

Potential damage may arise in the form of cracks or give rise to the incomplete extraction of the film as a consequence of a partial breakage. In our case, we applied a similar procedure that the one reported to attain self-standing mirrors embedding porous multilayers made of nanoparticles, which involved the cooling of the hybrid film down to the glass transition temperature of the infiltrated polymer. However, we could not successfully remove the nanocolumnar array from the glass substrate onto which it was directly deposited by doing this, the two types of imperfections mentioned above being present in the first self-standing flexible mirror we prepared. Based on our previous studies on flexible mirrors made from nanoparticle multilayers, we tried to use a packing of fine titanium oxide particles as an intermediate layer that was weakly bound to the substrate and could be easily separated from it by cooling.^[32,33] This feature would help to ease separation from the substrate, and should be smooth enough as to allow the deposition of regular arrays of nanocolumns by PV OAD onto it. As such layer is porous, it can be partially infiltrated by the polymer precursor. This approach was proven successful and a self-standing film could be attained following the procedure herein described and schematized in **Figure 1**. Analysis by field emission electron microscopy (FESEM) showed clear morphological differences between bare and infiltrated samples. **Figure 2a,b** display low-magnification images of a nanocolumnar DBR of alternated layers of titania and silica before and after being infiltrated and lifted off with the polymer of choice, PDMS, respectively. Two images attained zooming in the interface between the intermediate nanoparticle layer and the nanocolumns for both types of samples, displayed in **Figure 2c, d** show the modification of the morphology of the column and the nanoparticle layer after embedding the film within the polymer and demonstrate that there is a high

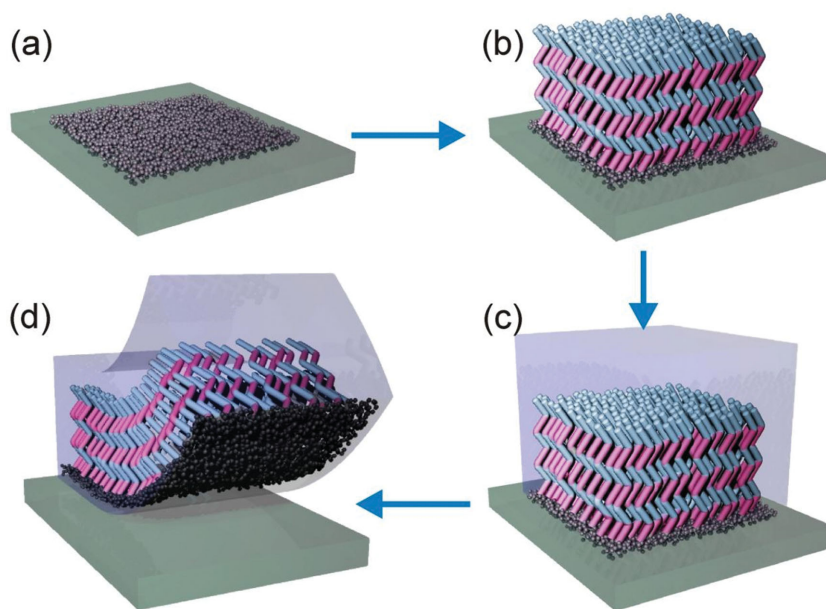


Figure 1. Scheme of the process that leads to a flexible hybrid film. a) A layer of nanoparticles of TiO_2 is deposited by spin coating; b) sequential deposition by PV OAD of a DBR; c) infiltration with PDMS; d) lifting-off process.

degree of infiltration of both of them. Please notice that the self-supported film also consists of an overlayer of PDMS that eases handling of the photonic crystal.

Periodic modulation of the refractive index in one direction, herein achieved through the alternated deposition of materials of different composition, gives rise to the opening of a photonic band gap. Light beams reflected at the interfaces of layers with different refractive index can interfere constructive or destructively. As a result, the propagation of electromagnetic waves through the photonic structure is forbidden for photons of certain energies. In fact, the phenomenon of constructive interference in the backwards direction leads to the appearance of the maximum in the reflectance spectrum characteristic of DBRs. A series of mirrors with similar columnar nanostructure but different lattice parameters, and hence optical properties, were prepared after this method. Five and a half periods of columnar layers were deposited onto a single titania nanoparticle intermediate layer. Effectively, it behaves as a six period 1D photonic crystal. **Figure 3** shows a series of pictures taken with a digital camera in which three structures reflecting dissimilar regions of the visible spectrum are depicted. In **Figure 3a**, we display images of the mirrors as originally deposited on nanoparticle titania-coated glass substrates, while **Figure 3b,c** show the same mirrors after being infiltrated with polymer before and after lifting them off, respectively. In all cases, a very intense reflection can be appreciated with the naked eye. The flexible films so prepared present no cracks or visible imperfections. Actually, the self-standing films preserve the optical quality of the infiltrated coating after removal from the substrate, which is a clear indication that the lifting-off process did not harm the photonic crystal structure. These can be readily appreciated in **Figure 4**, in which the series of reflectance spectra attained for each film depicted in **Figure 3** are plotted. The position of

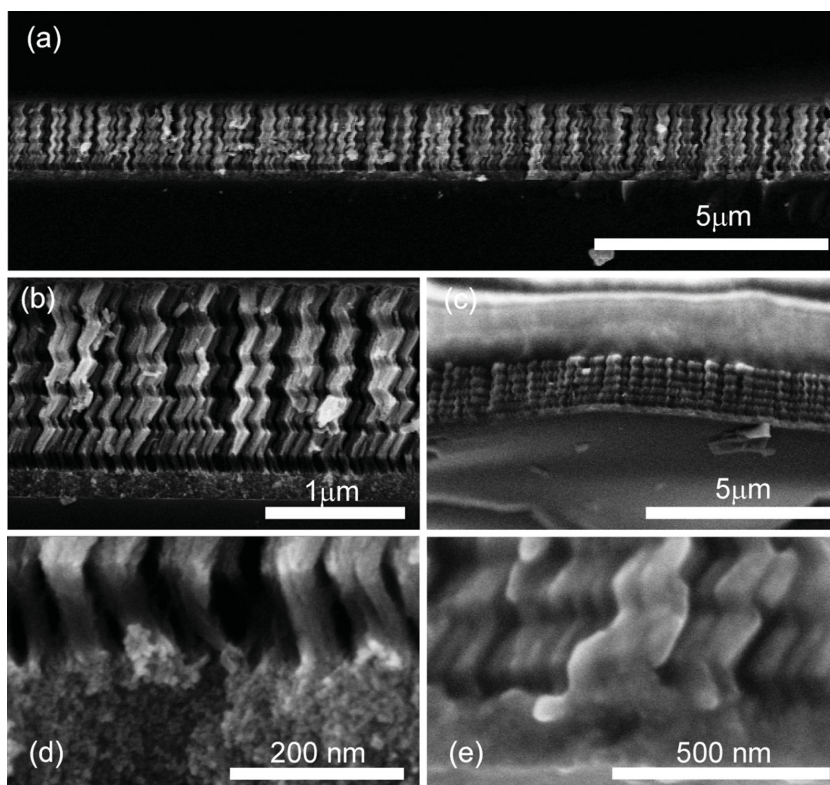


Figure 2. a, b) Cross section FESEM images of columnar 1DPC structure supported on silicon and c) self-standing structure. d, e) Zoomed images from images (b) and (c) showing the details of the nanocolumn–nanoparticle interface.

the normal incidence Bragg reflectance maximum, λ_B , can be approximated by the expression:

$$m\lambda_B = 2n_{\text{eff}}\Delta \quad (1)$$

where m is the diffraction order, Δ is the period or unit cell thickness, and n_{eff} is the effective refractive index that can be estimated using the expression:

$$n_{\text{eff}} = \frac{n_1 t_1 + n_2 t_2}{t_1 + t_2} \quad (2)$$

Being n_1 and n_2 the refractive indexes of the two types of constituent layers and t_1 and t_2 their thickness ($\Delta = t_1 + t_2$). After polymer infiltration, color changes are neatly observable in the case of the green and the orange samples. These are due to the redshift of the first-order Bragg peak maximum as a result of the increase of the average refractive index, as it can be derived from the approximate equation $\lambda_B = 2(t_1 n_1 + t_2 n_2)$, which results from combining (1) and (2).

A detailed analysis of the structure was performed by simulating the different reflectance spectra attained at the different stages of the preparation process. In order to do so, a code based on a combination of a transfer matrix approach to calculate the reflectance of each ensemble and a genetic algorithm to search for the optimum fitting was developed. Examples of the fittings attained are shown in Figure 4b as dotted lines. The small deviation from the theoretical spectrum indicates a very

low density of imperfections, which would give rise to diffuse scattering at the expense of diminishing the specular reflectance. From these we can estimate the filling fraction of polymer and the remaining porosity for each one of the layers in the flexible DBRs. In order to estimate the refractive index and fill factor (ff) of each component (metal oxide, polymer, air) within one specific layer, we made use of Bruggeman equation, which provides a relation between them and the average refractive index of the i th layer, n_i :

$$\frac{n_s^2 - n_i^2}{n_s^2 + 2n_i^2} ff_s + \frac{n_{\text{pol}}^2 - n_i^2}{n_{\text{pol}}^2 + 2n_i^2} ff_{\text{pol}} + \frac{n_{\text{vapor}}^2 - n_i^2}{n_{\text{vapor}}^2 + 2n_i^2} ff_{\text{vapor}} = 0 \quad (3)$$

where n_s , n_{pol} , and n_{void} (ff_s , ff_{pol} , and ff_{void}) are the refractive index (ff) of the metal oxide phase (SiO_2 or TiO_2) and of the polymer and vapor in the pores, respectively. This expression can be extended to as many components as necessary for more complex mesostructures. Assuming bulk values of $n_{\text{SiO}_2} = 1.45$, $n_{\text{TiO}_2} = 2.44$, and $n_{\text{pol}} = 1.43$, and the average refractive index of each type of infiltrated layer ($n_1 = 1.80$ and $n_2 = 1.43$, for TiO_2 and SiO_2 column-based layers, respectively) attained from the fittings, the average ff values attained are $ff_{\text{SiO}_2} = 60\%$, $ff_{\text{pol}} = 40\%$, and $ff_{\text{vapor}} = 0\%$ for the silica layers and $ff_{\text{TiO}_2} = 54\%$, $ff_{\text{pol}} = 5\%$, and $ff_{\text{vapor}} = 41\%$ for the titania layers. The intermediate nanoparticle layer presents $ff_{\text{TiO}_2} = 50\%$, $ff_{\text{pol}} = 10\%$, and $ff_{\text{vapor}} = 40\%$, and an average refractive index of 1.76.

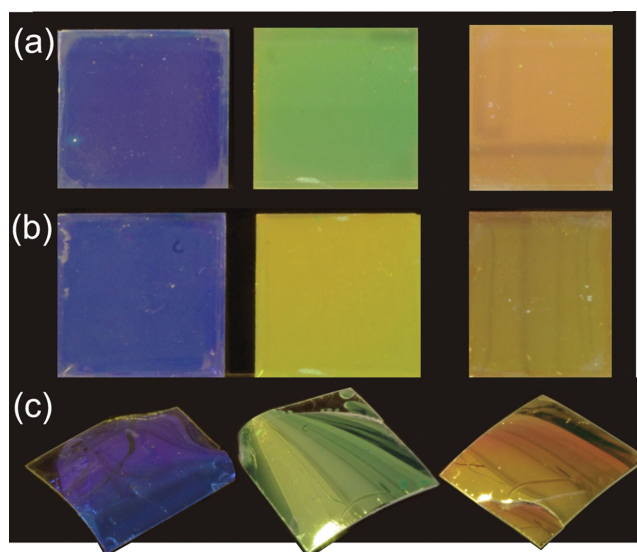


Figure 3. Photograph of nanocolumnar 1D photonic crystals with different unit cell size through different preparation stages. a) As-deposited onto glass substrate, b) after infiltration and PDMS polymerization, c) flexible and self-standing structures.

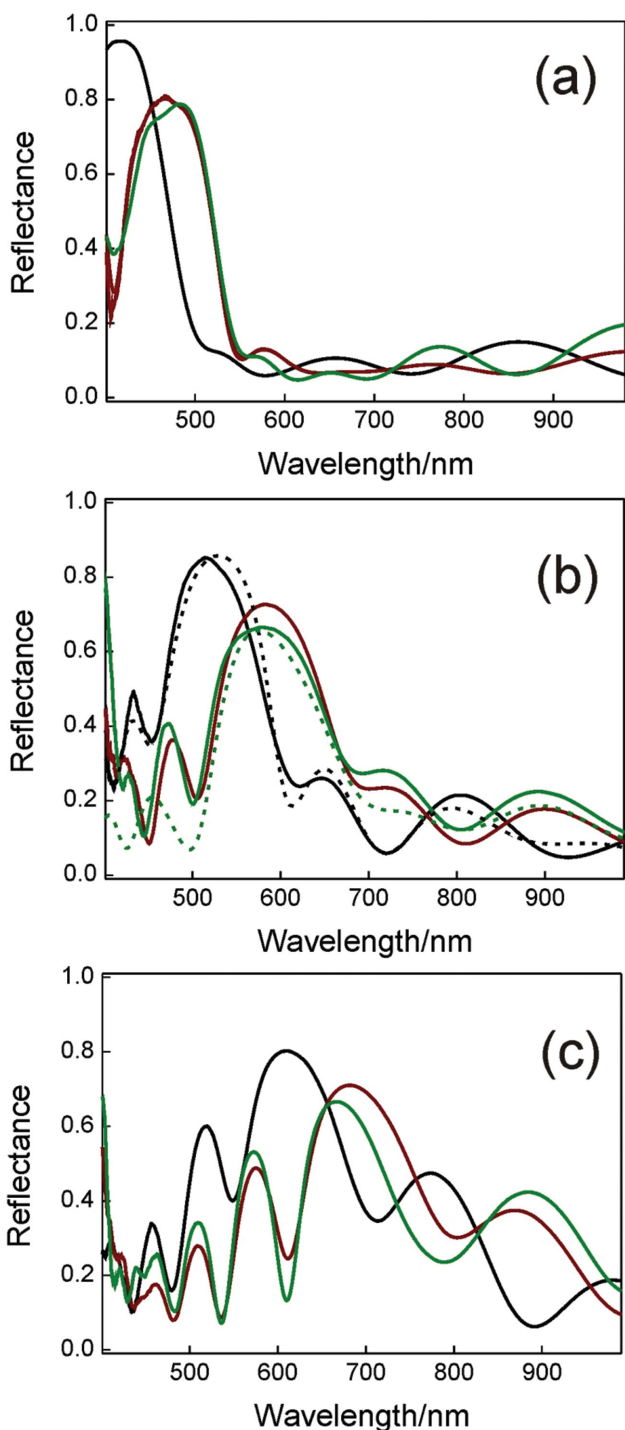


Figure 4. Reflectance spectra of three different DBRs. Different color lines indicate the different stages of the preparation stages: as deposited on glass substrate (black line), after infiltration and PDMS polymerization (dark red line) and self-standing film (dark green line). Figure 4b includes the theoretical fitting of the firstly deposited and the final self-standing mirror (black and green dashed lines, respectively).

These values are in good agreement with the porosities directly determined for individual layers of these two oxide nanostructures by water adsorption isotherms with a quartz crystal

monitor.^[27] The degree of polymer infiltration shows a gradual decrease as the layer under analysis is more deeply buried in the stack. This has a minor effect on the optical properties, both the primary maximum and the secondary reflectance lobes being slightly less intense than they would be in a homogeneously infiltrated multilayer. The dissimilar polymer ff observed between silica and titania layers has been previously observed in nanoparticle multilayers, and it very likely has its origin on the different affinity of PDMS for the two types of surfaces.^[34] On the other hand, it should be noticed that, in the case of the nanocolumnar structures, the degree of infiltration is higher than that reported for an all-nanoparticle-based 1D photonic crystal flexible films. A possible explanation for this effect is found in the much lower tortuosity of the void network in the former case.

The results herein reported serve to prove the proposed concept, i.e., that high quality flexible optical materials can be obtained from high dielectric contrast porous inorganic multilayers by infiltration of a polymer and using an intermediate nanoparticle layer to favor detachment from the substrate. We include in the supporting information a theoretical analysis of the evolution of the reflectance maximum versus the number of layers in the flexible mirror, which sets a threshold of nine periods (bilayers) to reach $R > 95\%$.

We have demonstrated that it is possible to create a highly reflecting frequency selective flexible mirror by infiltrating a DBR with a columnar nanostructure with an elastomer, preserving the high refractive index contrast of the original inorganic multilayered material and endowing it with mechanical properties that resemble those of the polymer. This is only possible through the use of an intermediate layer of nanoparticles that eases the lifting off the embedded coating from the substrate after cooling down the ensemble down to the glass transition temperature of the polymer. We believe this generic procedure could be extended to other inorganic nanostructures in order to maintain the optical performance of the inorganic structure in a self-standing film of improved mechanical properties. We foresee these types of materials will be of great interest for integration into bendable and stretchable optoelectronics, in which they would help to optimize the optical design of solar cells or light emitting devices.

Experimental Section

TiO₂-nanoparticulated layer were deposited onto 2.5 × 2.5 cm² substrates (glass slides or silicon wafers) from a colloidal suspension by spin coating (Laurell WS-400E-6NPP). Colloid synthesis was described elsewhere.^[35] Evaporation of the individual TiO₂ and SiO₂ layers was carried out in an electron bombardment evaporator by using TiO pellets (Kurt J. Lesker, titanium monoxide, 99,9%) or SiO₂ pellets (Sico Technology GmbH) as a target. Pretty homogenous multilayer films were obtained over the whole substrate area. The distance between the evaporation source and the substrate position was 80 cm. Deposition was carried out at room temperature. Stoichiometric and columnar layers of TiO₂ and SiO₂ were obtained by performing the evaporation in a chamber with an oxygen pressure of 10⁻⁴ torrs (this oxygen pressure is the source that allows us to deposit TiO₂ with the correct stoichiometry) by placing the substrates at a glancing zenithal angle $\alpha = 70^\circ$. These glancing geometries produce films with a tilted columnar microstructure. Successive and alternated layers of SiO₂ (1st, 3rd, 5th, etc.) and TiO₂ (2nd, 4th, and 6th) were prepared by changing the azimuthal orientation

of the substrate ϕ between 0° and 180° at each deposition. This procedure reduces the natural tendency of the nanocolumns to increase in width for higher layer thicknesses and to avoid undesirable light scattering effects associated to wider nanocolumns.^[25]

Polymerization within the Multilayer Interstices and Lifting Off: Elastomeric precursor and curing agent of PDMS (Sylgard 184, Dow Corning) were infiltrated depositing 0.5 g of the mix on top and then by spin coating (40 s, 700 rpm). After that, samples were maintained at room temperature during 24 h to facilitate the diffusion throughout the pore network. Next, PDMS was polymerized in a stove at 110° during 30 min. In order to lift off the flexible photonic structures, samples were immersed in liquid nitrogen (77 K). Then we allowed samples to warm up to temperature before lifting them off the substrate.

Optical Characterization: Reflectance spectra were performed using a Fourier transform infrared spectrophotometer (Bruker IFS-66 FTIR) attached to a microscope and operating in reflection mode with a 4X objective with 0.1 of numerical aperture (light cone angle $\pm 5.7^\circ$). Film images were acquired using a digital camera (Pentax Kx).

Structural Characterization: FESEM images of the multilayer films deposited onto silicon were taken by using a microscope Hitachi 5200 operating at 5 kV. Cross section microscope images of the self-standing multilayers were obtained by cutting samples with a sharp knife. A sputtered 6 nm layer of gold was deposited on top of the self-standing samples to minimize charging effects under microscope electron beam.

Acknowledgements

The research leading to these results has received funding from the European Research Council under the European Union's Seventh Framework Programme (FP7/2007–2013)/ERC grant agreement no. 307081 (POLIGHT), the Spanish Ministry of Economy and Competitiveness under grants MAT2011–23593, MAT2013–42900-P, and the Junta de Andalucía under grants FQM6900 and TEP8067. FESEM characterization was performed at CITIUS, and we are grateful for its support.

Received: July 28, 2014

Revised: September 15, 2014

Published online: February 17, 2015

- [1] G. Gustafsson, Y. Cao, G. M. Treacy, F. Klavetter, N. Colaneri, A. J. Heeger, *Nature* **1992**, 357, 477.
- [2] M. S. White, M. Kaltenbrunner, E. D. Glowacki, K. Gutnichenko, G. Kettlgruber, I. Graz, S. Aazou, C. Ulbricht, D. A. M. Egbe, M. C. Miron, Z. Major, M. C. Scharber, T. Sekitani, T. Someya, S. Bauer, N. S. Sariciftci, *Nat. Photonics* **2013**, 7, 811.
- [3] G. Li, R. Zhu, Y. Yang, *Nat. Photonics* **2012**, 6, 153.
- [4] F. C. Krebs, S. A. Gevorgyan, J. Alstrup, *J. Mater. Chem.* **2009**, 19, 5442.
- [5] L. S. Zhou, A. Wanga, S. C. Wu, J. Sun, S. Park, T. N. Jackson, *Appl. Phys. Lett.* **2006**, 88, 083502.
- [6] Q. F. Lin, H. T. Huang, Y. Jing, H. Y. Fu, P. C. Chang, D. D. Li, Y. Yao, Z. Y. Fan, *J. Mater. Chem. C* **2014**, 2, 1233.
- [7] J. Y. Lee, S. T. Connor, Y. Cui, P. Peumans, *Nano Lett.* **2008**, 8, 689.
- [8] M. Gross, D. C. Muller, H. G. Nothofer, U. Scherf, D. Neher, C. Brauchle, K. Meerholz, *Nature* **2000**, 405, 661.
- [9] K. Nomura, H. Ohta, A. Takagi, T. Kamiya, M. Mirano, H. Hosono, *Nature* **2004**, 432, 488.
- [10] F. Garnier, R. Hajlaoui, A. Yassar, P. Srivastava, *Science* **1994**, 265, 1684.
- [11] H. Chen, M. B. Mueller, K. J. Gilmore, G. G. Wallace, D. Li, *Adv. Mater.* **2008**, 20, 3557.
- [12] J. Lewis, *Mater. Today* **2006**, 9, 38.
- [13] K. J. Vahala, *Nature* **2003**, 424, 839.
- [14] S. Colodrero, A. Mihi, L. Haggman, M. Ocaña, G. Boschloo, A. Hagfeldt, H. Miguez, *Adv. Mater.* **2010**, 21, 764.
- [15] R. Betancur, P. Romero-Gomez, A. Martinez-Otero, X. Elias, M. Maymó, J. Martorell, *Nat. Photonics* **2013**, 7, 995.
- [16] W. J. Yu, L. Shen, P. Shen, Y. B. Long, H. W. Sun, W. Y. Chen, S. P. Ruan, *ACS Appl. Mater. Interfaces* **2014**, 6, 599.
- [17] J. Bailey, J. S. Sharp, *Eur. Phys. J. E* **2010**, 33, 41.
- [18] L. Frezza, M. Patrini, M. Liscidini, D. Comoretto, *J. Phys. Chem. C* **2011**, 115, 19939.
- [19] M. Kolle, A. Lethbridge, M. Kreysing, J. J. Baumberg, J. Aizenberg, P. Vukusic, *Adv. Mater.* **2013**, 25, 2239.
- [20] T. Druffel, N. Mandzy, M. Sunkara, E. Grulke, *Small* **2008**, 4, 459.
- [21] M. E. Calvo, J. R. C. Smirnov, H. Miguez, *J. Polym. Sci. B: Polym. Phys.* **2012**, 50, 945.
- [22] M. E. Calvo, O. Sanchez-Sobrado, G. Lozano, H. Miguez, *J. Mater. Chem.* **2009**, 19, 3144.
- [23] J. R. Castro Smirnov, M. E. Calvo, H. Miguez, *Adv. Funct. Mater.* **2013**, 23, 2805.
- [24] L. Gonzalez-Garcia, G. Lozano, A. Barranco, H. Miguez, A. R. Gonzalez-Elipe, *J. Mater. Chem.* **2010**, 20, 640.
- [25] M. Oliva-Ramirez, L. González-García, J. Parra-Barranco, F. Yubero, A. Barranco, A. R. González-Elipe, *ACS Appl. Mater. Interfaces* **2013**, 5, 6743.
- [26] M. J. Brett, M. M. Hawkeye, *Science* **2008**, 319, 1192.
- [27] R. Alvarez, C. Lopez-Santos, J. Parra-Barranco, V. Rico, A. Barranco, J. Cotrino, A. R. Gonzalez-Elipe, A. Palmero, *J. Vac. Sci. Technol. B* **2014**, 32, 041802.
- [28] L. González-García, J. Parra-Barranco, J. R. Sanchez-Valencia, A. Barranco, A. Borrás, A. R. González-Elipe, M. C. García-Gutierrez, J. J. Hernández, D. R. Rueda, T. A. Ezquerro, *Nanotechnology* **2012**, 23, 205701.
- [29] J. J. Steele, A. C. van Popta, M. M. Hawkeye, J. C. Sit, M. J. Brett, *Sens. Actuators B-Chem.* **2006**, 120, 2138.
- [30] M. F. Schubert, J. Xi, J. K. Kim, E. F. Schubert, *Appl. Phys. Lett.* **2007**, 90, 141115.
- [31] L. W. Bezuidenhout, N. Nazemifard, A. B. Jemere, D. J. Harrison, M. J. Brett, *Lab Chip* **2011**, 11, 1671.
- [32] O. Sanchez-Sobrado, M. E. Calvo, H. Miguez, *J. Mater. Chem.* **2010**, 20, 8240.
- [33] M. E. Calvo, H. Miguez, *Chem. Mater.* **2010**, 22, 3909.
- [34] M. Tsigge, T. Soddemann, S. B. Rempe, G. S. Grest, J. D. Kress, M. O. Robbins, S. W. Sides, M. J. Stevens, E. Webb, *J. Chem. Phys.* **2003**, 118, 5132.
- [35] S. D. Burnside, V. Shklover, C. Barbé, P. Comte, F. Arendse, K. Brooks, M. Grätzel, *Chem. Mater.* **1998**, 10, 2419.